SCIEPublish

Communication

Production and Calibration of a Lambertian Surface Based on Barium Sulfate ($BaSO_4$) for the Calibration of Multispectral Cameras

Daniel Carvalho Granemann [1], Adão Robson Elias [2,*], Henrique dos Santos Felipetto [2], Fernanda Sayuri Yoshino Watanabe [3] and Edson Luis Piroli [4]

[1] Department of Civil Engineering, Campus Apucarana-PR, Universidade Tecnológica Federal do Paraná, Apucarana 86812-460, Brazil; granemann@utfpr.edu.br (D.C.G.)

[2] Department of Surveying, Campus Pato Branco-PR, Universidade Tecnológica Federal do Paraná, Pato Branco 85503-390, Brazil; felipetto@utfpr.edu.br (H.d.S.F.)

[3] Department of Cartographic Engineering, College of Science and Technology (FCT), Campus Presidente Prudente-SP, Universidade Estadual Paulista Júlio de Mesquita Filho, Presidente Prudente 19060-900, Brazil; fernanda.watanabe@unesp.br (F.S.Y.W.)

[4] College of Science, Technology and Education (FCTE), Campus Ourinhos-SP, Universidade Estadual Paulista Júlio de Mesquita Filho, Ourinhos 19903-302, Brazil; edson.piroli@unesp.br (E.L.P.)

* Corresponding author. E-mail: robsonelias@utfpr.edu.br (A.R.E.)

Received: 26 April 2025; Accepted: 19 June 2025; Available online: 26 June 2025

ABSTRACT: Drones, or unmanned aerial vehicles (UAVs), are increasingly utilized across diverse fields such as agriculture, environmental analysis, and engineering due to their ability to capture high-quality multispectral imagery. To ensure the accuracy of these images, radiometric calibration of onboard multispectral cameras is essential. This study aimed to develop and calibrate a low-cost Lambertian surface using barium sulfate ($BaSO_4$) for radiometric calibration of UAV-mounted multispectral cameras. A stainless steel mold was designed to compact $BaSO_4$, and the resulting surface was calibrated using an ASD FieldSpec HandHeld UV/NIR spectroradiometer and a Spectralon plate as the reference standard. Results showed a strong correlation (Pearson's r = 0.9988) between the $BaSO_4$ surface and the Spectralon plate, confirming that the $BaSO_4$-based surface is a cost-effective alternative for producing diffuse Lambertian surfaces with performance comparable to the standard.

Keywords: UAV; Multispectral; Surface; Diffuse

1. Introduction

Since the late 1960s, Brazil has advanced remote sensing capabilities through the National Institute for Space Research (INPE), establishing infrastructure and training professionals to apply these techniques effectively [1]. Remote sensing enables non-contact data collection from the Earth's surface by capturing reflected or emitted electromagnetic energy, which is transformed into actionable information about the target area. Applications include environmental monitoring, agriculture, and urban planning, among others.

Remote sensors, mounted on platforms such as aircraft, unmanned aerial vehicles (UAVs), or satellites, convert electromagnetic energy into signals that reveal insights about the study site. When electromagnetic energy interacts with surfaces, it may be reflected, absorbed, or transmitted, depending on the surface's physical and chemical properties, the wavelength of the incident radiation, and the angle of incidence. These interactions produce unique spectral signatures for different materials (e.g., vegetation, soil, water), enabling their identification in multispectral imagery, as shown in Figure 1.

https://doi.org/10.70322/dav.2025.10012

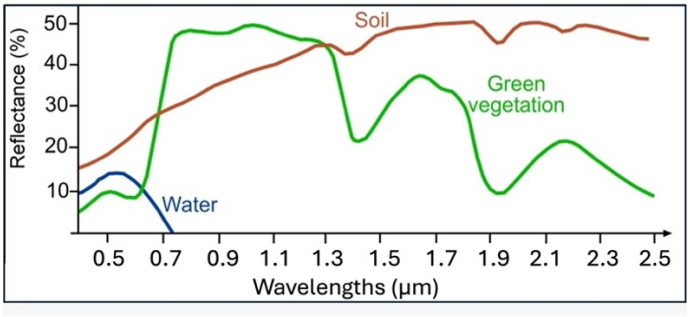

Figure 1. Spectral signatures of vegetation, soil and water [2].

Therefore, accurate interpretation of multispectral images requires precise calibration of the cameras to ensure reliable data. Calibration involves using a Lambertian surface—A surface with ideal diffuse reflectance that exhibits uniform radiance regardless of viewing angle (Figure 2).

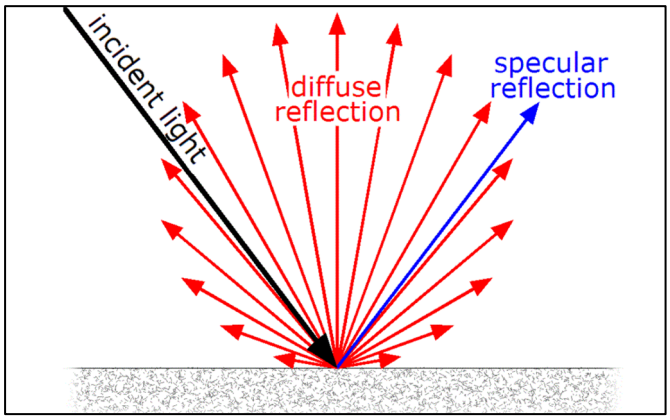

Figure 2. Radiation intensity measured as a function of the viewing angle [3].

According to [4], typically, an integrating sphere coated with highly reflective materials like magnesium oxide, barium sulfate ($BaSO_4$), or polytetrafluoroethylene (PTFE) is used to measure diffuse reflectance. Spectralon, a fluoropolymer with near-perfect diffuse reflectance (99%) and exceptional whiteness, is the standard material for such calibrations [5] but is costly.

As UAVs expand in popularity and application, the need for affordable and effective calibration methods grows. Multispectral camera calibration enhances image quality, reduces processing time, and improves integration with systems like Global Navigation Satellite Systems (GNSS), leading to greater efficiency and lower operational costs [6]. Recent comprehensive studies have also emphasized the critical role of radiometric calibration in ensuring data reliability for UAV-based remote sensing applications. For instance, ref. [7] provide practical guidance for environmental mapping using UAS, highlighting the fundamental importance of calibration surfaces to achieve consistent and trustworthy reflectance data under varying field conditions. However, existing calibration systems are often expensive or inaccessible, limiting their adoption.

Therefore, this study is of particular importance, given that the calibration of cameras on board drones is currently expensive or does not yet have an adequate system with affordable prices to ensure the best image acquisition, which would allow for accurate data on the object and/or phenomenon under study.

The main objective was to develop a low-cost Lambertian surface using $BaSO_4$ for calibrating UAV-mounted multispectral cameras and validate its performance against a Spectralon plate, the industry standard for calibrating such cameras.

2. Materials and Methods

First, a stainless steel part was developed, a material resistant to oxidation, for compacting $BaSO_4$, a low-cost chemical material, white in color and not harmful to health, which can be handled without the use of personal protective equipment (PPE). The design of the part, front and top view, is shown in Figure 3.

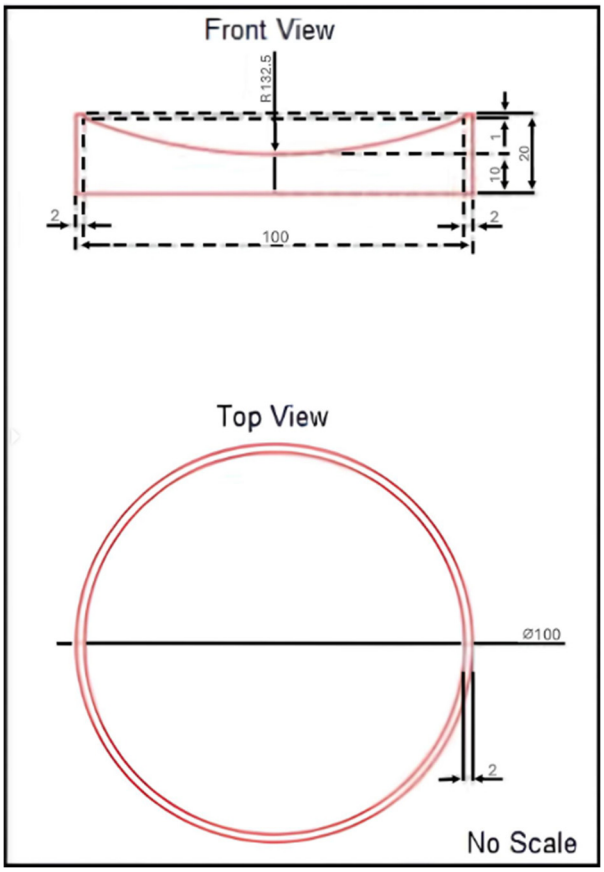

Figure 3. Stainless steel part design—Millimeter units.

In Figure 4, you can see the machined stainless steel part, according to the design and dimensions shown in Figure 3.

Figure 4. Machined stainless steel part.

The part was then filled with $BaSO_4$ (Figure 5) up to the upper edge, later adjusted in the hydraulic-mechanical press (Figure 6a)—Belonging to the Concrete Laboratory of the Federal Technological University of Paraná—Pato Branco Campus. After adjusting the stainless steel part in the press (Figure 6b), a pressure of 100 tons-force (tf) was applied (Figure 6c) for compaction, equivalent to 124,861.676 N/mm^2. The tests carried out proved that this was the pressure considered ideal since the compacted material did not present cracks or superficial fissures, which is important for the homogenization of the $BaSO_4$ in the stainless steel part.

Figure 5. Stainless steel part filled with $BaSO_4$.

(**a**) (**b**) (**c**)

Figure 6. (**a**) Adjustment of the part in the hydraulic press. (**b**). Stainless steel part adjusted in the hydraulic press. (**c**) Pressure of 100 tf for compacting $BaSO_4$.

The surface of the compacted $BaSO_4$ presented irregularities due to the removal of the upper part of the part (Figure 7). Sandpaper with grits 2000 and 3000 was used to remove these imperfections in order to obtain a homogeneous finish free from compression marks (Figure 8) in the hydraulic press, which could interfere with the final texture of the Lambertian surface.

Figure 7. Irregularities on the surface of compacted $BaSO_4$.

Figure 8. Irregularities on the $BaSO_4$ surface removed with 2000 and 3000 grit water sandpaper.

The next step was the calibration of the compressed $BaSO_4$, using the ASD FieldSpec HandHeld UV/NIR spectroradiometer and the Labsphere Spectralon plate (25 × 25) cm (Figure 9), both belonging to the Sensor Integration Laboratory of the Department of Certography of the Universidade Estadual Paulista Júlio de Mesquita Filho (UNESP)—Presidente Prudente Campus, state of São Paulo, Brazil.

Figure 9. Spectralon plate [8].

The calibration was performed in a dark room whose entire interior was painted matte black so that there would be no reflection of the light source in the environment nor interference from external light, with only one light source falling on the Spectralon plate (Figure 10), which was maintained throughout the process with the same intensity and angle, in order to provide results under the same conditions for the objects used in the experiment. In addition, care was taken not to remain close to the equipment since reflective surfaces could interfere with the spectroradiometer reading process. This equipment provides results in the electromagnetic spectrum range (Figure 11) between wavelengths 325 to 1075 nm, that is, from ultraviolet to near infrared.

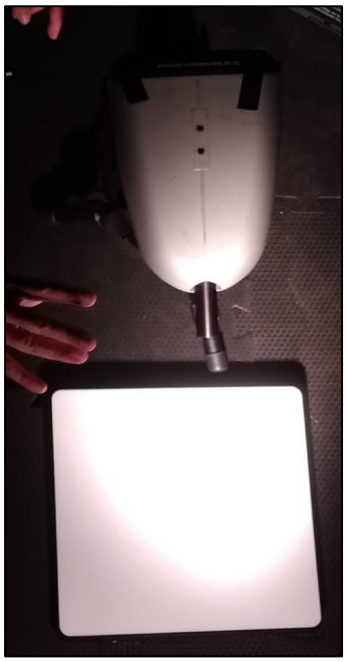

Figure 10. Light source on the Spectralon plate.

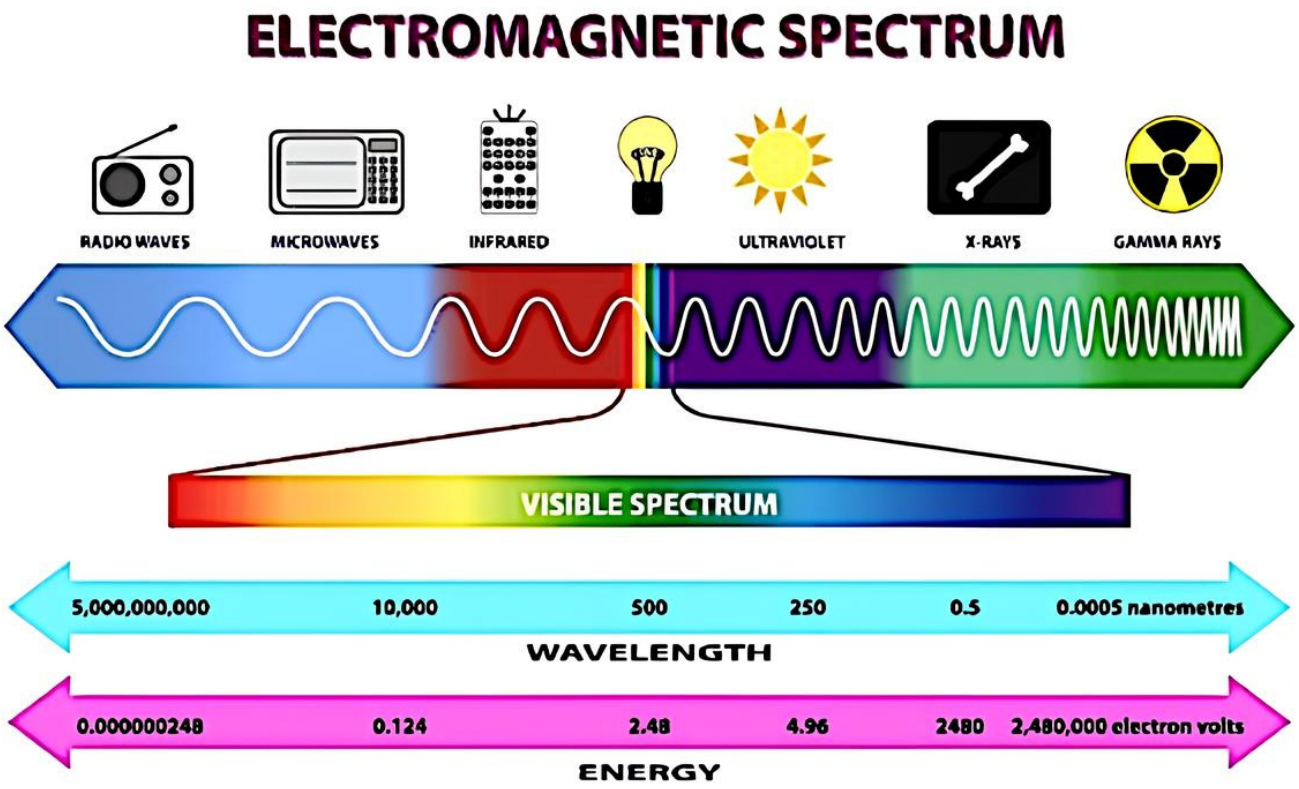

Figure 11. Electromagnetic spectrum [9].

The spectroradiometer, with a 1º IFOV (Instantaneous Field of View) lens on the Spectralon plate and $BaSO_4$, was configured using the Malvern Panalytical RS3 software to perform 10 reading sessions, capturing the reflectance for each wavelength. First, the readings were performed on the Spectralon plate (Figure 9), which was adopted as the standard for the other observations, and then on the $BaSO_4$ compressed in the stainless steel piece (Figure 12).

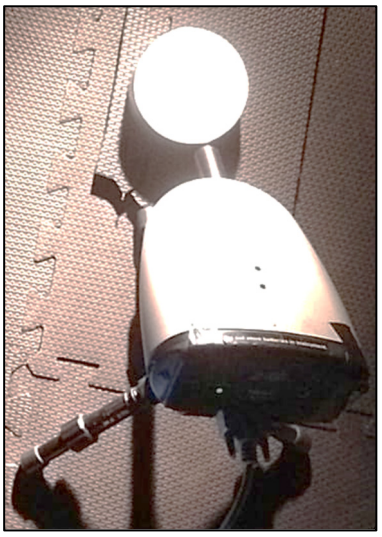

Figure 12. Spectroradiometer making observations on $BaSO_4$.

After the observations were performed, the data obtained were transferred to the computer using the ASD Viewspec Pro software, version 6.2. The raw data were corrected using equations to calculate the elements needed to obtain the corrected reading values for the Spectralon plate and $BaSO_4$. For this step, the data were tabulated in a spreadsheet, and the averages between the 10 reading sessions for each wavelength were calculated. Next, the reflectance correction factors were calculated for each average between the Spectralon plate and $BaSO_4$ (Equation (1)), adapted from [10]:

$$Fc = \frac{M_S}{M_P} \quad (1)$$

where:
Fc—correction factor;
M_S—average between Spectralon readings for each wavelength;
Mp—average between barium sulfate readings for each wavelength.

Therefore, to obtain the corrected readings of the observed electromagnetic spectrum (325 to 1075 nm) for $BaSO_4$, Equation (2) [10] is adopted:

$$C = M_P \cdot F_C \quad (2)$$

where:
C—corrected reading for the wavelengths obtained for $BaSO_4$.

To calculate the reflectance (R), Equation (3) is used.

$$R = \frac{F_{CMP}}{M_S} \quad (3)$$

where:
F_{CMP}—correction factor of the averages between the $BaSO_4$ readings.

3. Results and Discussions

Since the tabulated wavelengths are listed every 1 nm, it is impossible to reproduce the data in full since they total 752 lines of the spreadsheet. Therefore, a partial reproduction of these data is made every 50 nm. Table 1 presents the means and respective standard deviations for the dimensionless reflectance factors of the Spectralon plate and $BaSO_4$, as a function of the wavelengths, in the range of 350 to 1050 nm.

Table 1. Reflectance factors for wavelengths.

Wavelength (nm)	Averages of Reflectance Factors		Standard Deviations *	
	Spectralon	$BaSO_4$	σ_S	σ_B
350	0.000010483	0.000005812		
400	0.000066462	0.000036626		
450	0.000185969	0.000107591		
500	0.000396167	0.000242135		
550	0.000693409	0.000440373		
600	0.001047372	0.000692338		
650	0.001402429	0.000953264	±0.001148534	±0.000862482
700	0.001761664	0.001229098		
800	0.002357676	0.001707109		
850	0.002543110	0.001867201		
900	0.002807288	0.002088002		
950	0.003055473	0.002301816		
1000	0.003174858	0.002403606		
1050	0.003232645	0.002510302		

* Standard deviations: σ_S—Spectralon; σ_B—$BaSO_4$.

From the data in Table 1, the graph shown in Figure 13 was obtained.

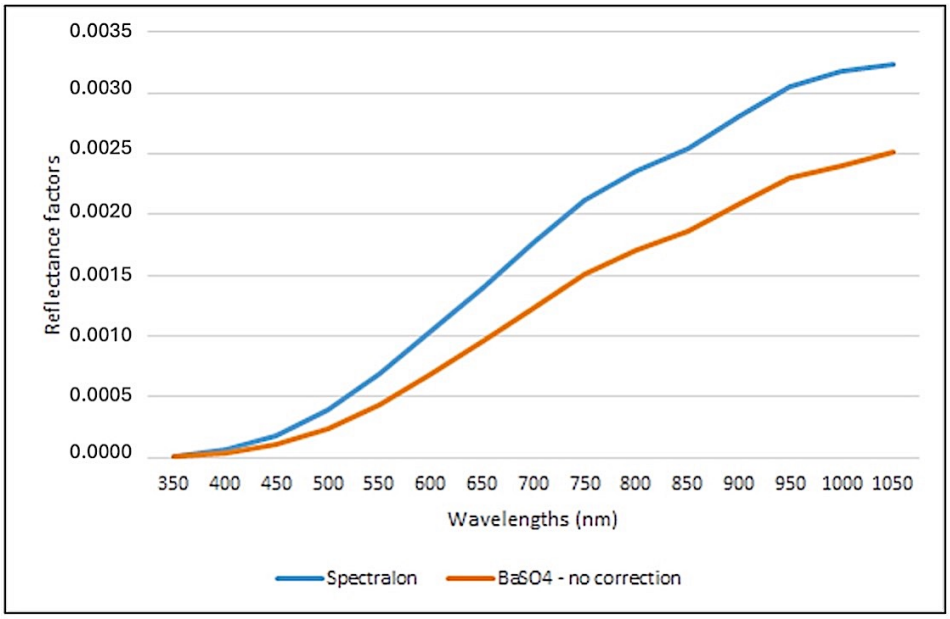

Figure 13. Averages of the reflectance factors of Spectralon and $BaSO_4$ as a function of wavelengths.

Although the corrections for the reflectance factors have not yet been applied, Figure 13 shows a direct relationship between the Spectralon and $BaSO_4$ graphs, with a value of 0.9988 for Pearson's correlation, i.e., a strong linear relationship, according to [11]. It is also possible to infer from the data, reproduced in part in Table 1 and observed in Figure 13, that the maximum difference between these is 0.00071 and the minimum is −0.000004, which, due to its magnitude, ends up corroborating the correlation above.

By applying Equation (3), it is possible to calculate the *R*-value of $BaSO_4$, even without correction, in order to compare it with the R of the Spectralon plate, whose value is 1 (Figure 14).

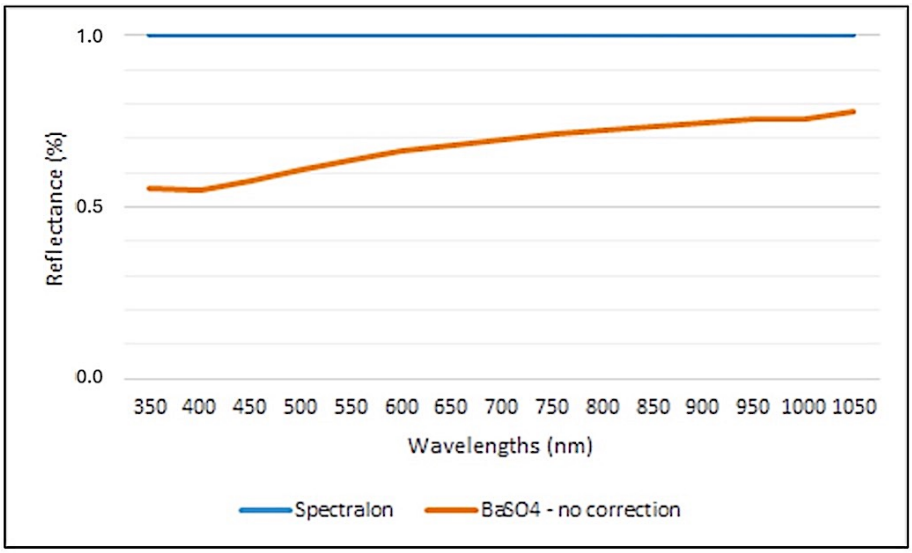

Figure 14. Reflectance of Spectralon and $BaSO_4$ plate—Without correction—as a function of wavelengths.

Since the Spectralon plate is the standard for obtaining R, there is a correlation of 0.9620 between the reflectances of these two elements, that is, a strong linear relationship, according to [11], which was expected, given that Figure 13 already demonstrated this trend.

Therefore, in order to have a perfect relationship between these elements, the corrections for the reflectance factors of $BaSO_4$ were calculated, given by Equations (1) and (2), presented in Table 2.

Table 2. Corrections for the reflectance factors of $BaSO_4$.

Wavelength (nm)	$BaSO_4$ (No Correction)	Correction Factors (FC)	$BaSO_4$ (Corrected)
350	0.000005812	1.803586628	0.000010483
400	0.000036626	1.814606393	0.000066462
450	0.000107591	1.728482347	0.000185969
500	0.000242135	1.636141962	0.000396167
550	0.000440373	1.57459658	0.000693409
600	0.000692338	1.512804132	0.001047372
650	0.000953264	1.471186638	0.001402429
700	0.001229098	1.433298616	0.001761664
800	0.001707109	1.40446804	0.002122530
850	0.001867201	1.381092323	0.002357676
900	0.002088002	1.361990888	0.002543110
950	0.002301816	1.344485405	0.002807288
1000	0.002403606	1.327418407	0.003055473
1050	0.002510302	0.002510302	0.003174858

Equation (1) provides the values for the CFs, while Equation (2) allows the calculation of the corrected reflectance factors for $BaSO_4$. After that, these factors were compared with those of the Spectralon plate (Table 3) in order to verify the possibility of $BaSO_4$ being adopted as a Lambertian surface.

Table 3. Comparison between reflectance factors of Spectralon and $BaSO_4$.

Wavelength (nm)	Spectralon	$BaSO_4$ (Corrected)	Differences
350	0.000010483	0.000010483	0.000000000
400	0.000066462	0.000066462	0.000000000
450	0.000185969	0.000185969	0.000000000
500	0.000396167	0.000396167	0.000000000
550	0.000693409	0.000693409	0.000000000
600	0.001047372	0.001047372	0.000000000
650	0.001402429	0.001402429	0.000000000
700	0.001761664	0.001761664	0.000000000

800	0.002122530	0.002122530	0.000000000
850	0.002357676	0.002357676	0.000000000
900	0.002543110	0.002543110	0.000000000
950	0.002807288	0.002807288	0.000000000
1000	0.003055473	0.003055473	0.000000000
1050	0.003174858	0.003174858	0.000000000

The differences observed in Table 3 indicate that $BaSO_4$ can be used as a Lambertian surface, as it presents results identical to the Spectralon plate, as shown in Figure 15.

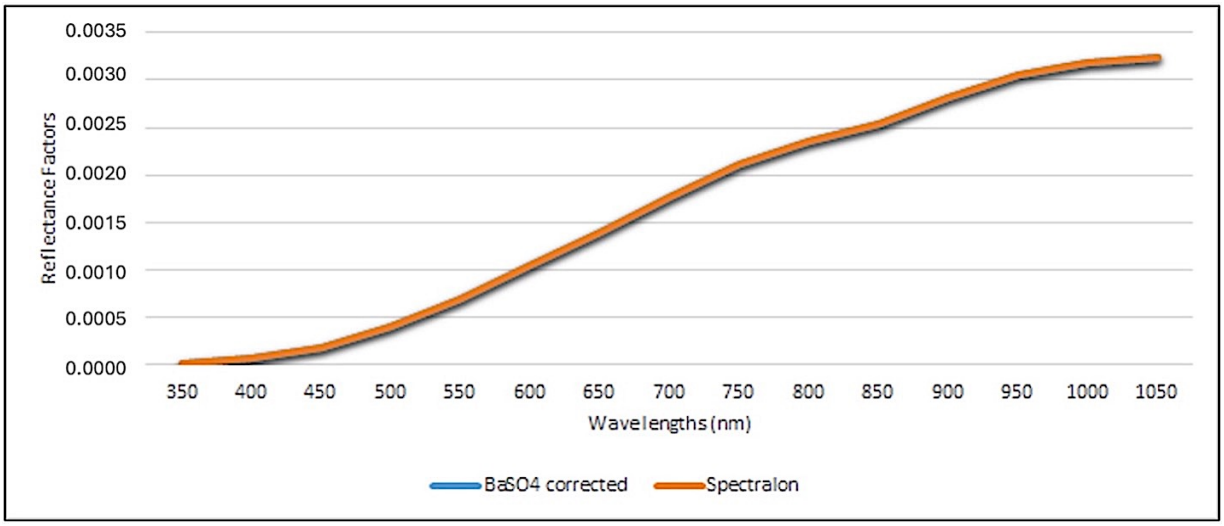

Figure 15. Reflectance factors of Spectralon and corrected BaSO4.

The overlap of the graphs of Spectralon and corrected $BaSO_4$ demonstrate the perfect agreement between their reflectance factors, corroborating what was stated in the previous paragraph.

In turn, Figure 16 shows the graphs of the reflectances of Spectralon and $BaSO_4$, which, as previously stated, were expected to overlap with R equal to 1 since there is a strong linear correlation between them.

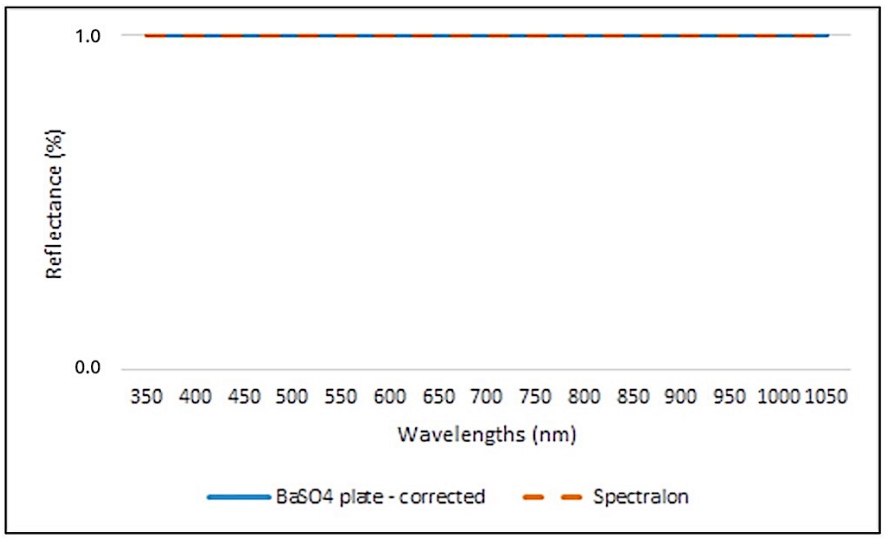

Figure 16. Reflectance of the Spectralon and $BaSO_4$ plate—corrected—as a function of wavelengths.

4. Conclusions

The development and calibration of a low-cost Lambertian surface using barium sulfate ($BaSO_4$) demonstrated performance comparable to the industry-standard Spectralon plate, with a Pearson's correlation of 0.9988. This $BaSO_4$-based surface offers an economically viable alternative for radiometric calibration of multispectral cameras mounted on unmanned aerial vehicles (UAVs), enabling high-quality image acquisition at reduced costs.

To further validate the $BaSO_4$ surface, additional testing with diverse multispectral sensors under varied field conditions is recommended. Such studies will confirm its reliability across real-world applications and environmental settings, potentially broadening its adoption in remote sensing workflows.

Furthermore, the approach developed in this study can be adapted for the calibration of different types of optical sensors, including hyperspectral cameras and portable field spectrometers, provided that the spectral and geometric specifications of each device are considered. Likewise, its application under varying operational conditions—such as changes in natural lighting, ambient temperature, or relative humidity—should be evaluated in future investigations to validate the stability and robustness of the $BaSO_4$ surface in realistic data acquisition scenarios.

Acknowledgements

To my colleague Gabriela Zanchetta, a PhD student in the Postgraduate Course in Cartographic Sciences at UNESP—Presidente Prudente, for her support and guidance in using the ASD FieldSpec HandHeld UV/NIR spectroradiometer and Spectralon plate. To Fábio Larini, owner of the company WD Tron, for his support in the project. To the Brazilian Center for UAVs for Aerolifting—NUBRAVA, for his support of the project.

Author Contributions

Conceptualization and Writing, D.C.G.; Methodology and Supervision, A.R.E.; Software, F.S.Y.W.; Review, H.d.S.F., E.L.P.

Ethics Statement

Not applicable.

Informed Consent Statement

Not applicable.

Data Availability Statement

The data supporting the findings of this study are available from upon reasonable request.

Funding

This research received no external funding.

Competing Interest Statement

The authors declare that they have no known competing financial interests or personal relationships that could have influenced the work reported in this article.

AI Usage Statement

During the preparation of this work, the authors used ChatGPT-4 to improve readability and language. After using this tool/service, the authors reviewed and edited the content as necessary and assume full responsibility for the content of the publication.

References

1. NOVO EMLM. Introdução ao sensoriamento remoto. Divisão de Processamento de Imagens. Instituto Nacional de Pesquisas Espaciais. São José dos Campos, 2001. Available online: http://www.dpi.inpe.br/Miguel/AlunosPG/Jarvis/SR_DPI7.pdf (accessed on 18 May 2024).
2. Campbell JB, Wynne RH. *Introduction to Remote Sensing*, 5th ed.; Guildford Press: New York, NY, USA, 2011.
3. UFRGS—CENTRO DE REFERÊNCIA PARA O ENSINO DE FÍSICA. Confusão entre reflexão especular e difusa, 2021. Available online: https://cref.if.ufrgs.br/?contact-pergunta=confusao-entre-reflexao-especular-e-difusa (accessed on 15 April 2025).
4. Souza MA, Silva EM, Gomes JFS, Guedes MB, Alvarenga AD. Implantação de um sistema de medição em reflectância espectral difusa. 7º Congresso Brasileiro de Metrologia. Ouro Preto, MG. 2013. Available online: file:///C:/Users/Daniel/Downloads/Metrologia2013_Muriel-EsferaIntegradora.pdf (accessed on 18 June 2024).

5. LABSPHERE —Spectralon® diffuse reflectance standards—Unequalled Lambertian reflectance from 250–2500 nm. Available online: https://www.labsphere.com/product/Spectralon-diffuse-reflectance-standards (accessed on 5 March 2025).
6. AERO—Quais são os 7 benefícios da calibração de câmeras em drones? 2023. Available online: https://aeroengenharia.com/glossario/quais-sao-os-7-beneficios-da-calibracao-de-cameras-em-drones/#:~:text=A%20calibra%C3%A7%C3%A3o%20das%20c%C3%A2meras%20dos%20drones%20tamb%C3%A9m%20contribui%20para%20aumentar,e%20a%20consist%C3%AAncia%20dos%20resultados (accessed on 18 June 2024).
7. Tmušić G, Manfreda S, Aasen H, James MR, Gonçalves G, Ben-Dor E, et al. Current Practices in UAS-Based Environmental Monitoring. *Remote Sens.* **2020**, *12*, 1001. Available online: https://doi.org/10.3390/rs12061001 (accessed on 6 June 2025).
8. UNESP. Placa de Spectralon. Laboratório de integração de sensores. Curso de pós-graduação em ciências cartográficas. Universidade Estadual Paulista Júlio de Mesquita Filho, Presidente Prudente, 2025.
9. Franciolle M. O que é Espectro Eletromagnético? Gaia Ciência, 2022. Available online: https://gaiaciencia.com.br/o-que-e-espectro-eletromagnetico-espaco--fisica (accessed on 15 April 2025).
10. Jensen JR. *Sensoriamento remoto do ambiente: Uma perspectiva em recursos terrestres*; Epiphanio JCN, Formaggio AR, Santos AR, Rudorff BFT, Almeida CM, Galvão LS, Translators; Parêntese: São José dos Campos, Brazil, 2009; p. 598.
11. Rumsey DJ. What is r value correlation? Statistics for dummies. 2023. Available online: https://www.dummies.com/article/academics-the-arts/math/statistics/how-to-interpret-a-correlation-coefficient-r-169792 (accessed on 27 March 2025).